A Laser-Cooled, High Density Positron Plasma[§]

B.M. Jelenković[†], A.S. Newbury[*], J.J. Bollinger, T.B.Mitchell[‡] and W.M. Itano

Time and Frequency Division, NIST, Boulder, CO 80305

Abstract. We present results on trapping and cooling of positrons in a Penning trap. Up to a few thousand positrons are trapped and sympathetically cooled through Coulomb collisions (sympathetic cooling) with laser-cooled $^9Be^+$ ions. By imaging the $^9Be^+$ laser-induced fluorescence, we observe centrifugal separation of the $^9Be^+$ ions and the positrons, with the positrons coalescing into a column along the trap axis. This indicates the positrons have the same rotation frequency and comparable density ($\sim 4 \times 10^9$ cm^{-3}) as the $^9Be^+$ ions, and places an upper limit of approximately 5 K on the positron temperature of motion parallel to the magnetic field. The measured positron lifetime is > 8 days in our room temperature vacuum of 10^{-8} Pa.

I INTRODUCTION

This paper presents experimental results on the capture, storage and cooling of positrons in a Penning trap that simultaneously contains laser-cooled $^9Be^+$ ions. The experimental work follows previous discussions and simulations of trapping and sympathetic cooling of positrons via Coulomb collisions with cold $^9Be^+$ ions [1,2]. Similar and somewhat more detailed discussions are given in [3]. Cold positron plasmas are useful as a source for cold beams of high brightness [4,5]. In addition cold positron plasmas are useful for studies of positron-normal-matter interactions, such as the study of resonances in low-energy positron annihilation on molecules [4], for production of a plasma whose modes must be treated quantum mechanically [1,6], and for formation of antihydrogen by passing cold antiprotons through a reservoir of cold positrons [7,8].

Several groups have successfully trapped positrons in electromagnetic traps. Positrons have been trapped using resistive cooling of the positrons [9], by ramping the trap electrostatic potential [10], and in a magnetic-mirror configuration by electron cyclotron-resonance heating [11]. Recent experiments by Gabrielse and co-workers [8,12,13] have successfully trapped more than 10^6 positrons in a cryogenic trap in 1 hour through a method where positronium in a high Rydberg state created

CP606, *Non-Neutral Plasma Physics IV*, edited by F. Anderegg et al.
2002 American Institute of Physics 0-7354-0050-4

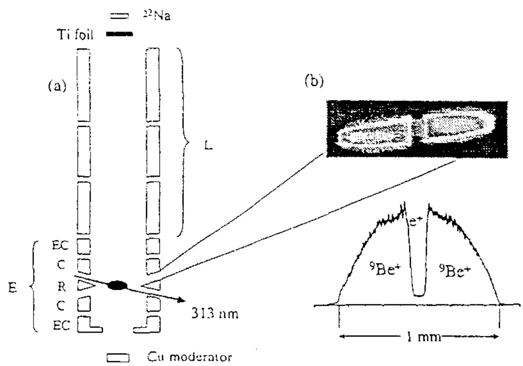

FIGURE 1. (a) Schematic diagram of the load and experimental cylindrical Penning traps; EC=end cap, C=compensation, R=ring of the experimental trap. (b) Two species $^9Be^+$ - e^+ plasma: camera image (top) and radial variation of fluorescence signal integrated over z (bottom).

on the surface of the moderator is field-ionized in the trap. Surko and co-workers [4,5,14–16], using a 90 mCi positron source, report the largest number of trapped positrons ($\sim 3 \times 10^8$) with a trapping rate of 3×10^8 positrons in 8 minutes and a trapping efficiency greater than 25 % of the moderated positrons. In these experiments trapping was achieved through collisions with a room-temperature buffer gas of N_2. In this paper we discuss the results of simultaneously trapping and cooling positrons with laser-cooled $^9Be^+$ ions. We observe centrifugal separation of the positrons and $^9Be^+$ ions, which enables us to determine the positron density and place a rough upper bound on the positron temperature.

II EXPERIMENTAL SETUP

The Penning trap, along with the positron source and positron moderator are shown in Fig. 1(a). The stack of cylindrical electrodes (10 mm in diameter, 60 mm long) forms two Penning traps, in a 6 T magnetic field. The top, load (L) trap was used to create $^9Be^+$ ion plasmas by ionizing neutral ^9Be atoms sublimated from a heated ^9Be filament. The $^9Be^+$ ions are transferred to the lower, experimental (E) trap for experimentation. In a single load-transfer cycle we can store over one million ions. An axisymmetric, nearly quadratic trapping potential is generated by biasing the ring of the experimental trap to a negative voltage V_R and adjacent compensation electrodes to $V_C = 0.9\times V_R$. For V_R= -100 V, and for the endcap voltage $V_{EC} = 0$ the single particle axial frequency for $^9Be^+$ ions is $\omega_z/2\pi$=870 kHz, and the magnetron frequency is $\omega_m/2\pi$=35 kHz.

The ions were cooled by a laser beam tuned $\sim$ 10 MHz lower than a hyperfine-Zeeman component of the $2s^2S_{1/2} \rightarrow 2p^2P_{3/2}$ resonance in $^9Be^+$ at 313 nm [17]. The laser beam was directed through the trap, intersecting the ion plasma on the side receding from the laser beam due to the plasma rotation. As shown in Fig. 1(a) the beam entered the trap between the upper compensation and ring electrodes, passed through the trap center, and exited through the gap between the ring and lower compensation electrode, making an 11° angle with the horizontal (x-y) plane. Based on measurements performed in previous experiments [17–19] we expect $T_\perp \leq T_\parallel \leq 100$ mK, where $T_\perp$ and $T_\parallel$ describe the velocity distributions in the direction perpendicular and parallel to the trap axis (z axis).

An ion plasma in thermal equilibrium at these cryogenic temperatures is a uniform-density plasma with a rigid-body rotation frequency ω_r in the range $\omega_m < \omega_r < \Omega - \omega_m$, where $\Omega = 10.2$ MHz is the ion cyclotron frequency. We used a rotating electric field perturbation to control ω_r [20]. The ion density is constant within the plasma and is given by $n_0 = 2\epsilon_0 m\omega_r(\Omega - \omega_r)/q^2$, where q and m are the charge and mass of an ion, and ϵ_0 is the permittivity of the vacuum. Since the trapping potential is quadratic near the trap center, the plasma has the shape of a spheroid whose aspect ratio, $\alpha = z_0/r_0$, depends on ω_r. Here $2z_0$ and $2r_0$ are the axial and radial extents of the plasma spheroid. Low rotation ($\omega_r \sim \omega_m$) results in an oblate spheroid of large radius. Increasing ω_r increases the Lorentz force due to the plasma rotation through the magnetic field, which in turn increases α and n_0. At $\omega_r = \Omega/2$ (Brillouin limit) the ion plasma attains its maximum aspect ratio and density. For $^9Be^+$ ions at 6 T the maximum ion density is 1.1×10^{10} cm^{-3}. Side-view images of the $^9Be^+$ plasma spheroid were produced by an f/5 imaging system that sends 313 nm photons scattered in a direction 11° above the z = 0 plane of the trap onto the photocathode of a photon-counting imaging detector.

The source for the positrons is a 2 mCi ^{22}Na source with an active diameter of ~1 mm. The source is placed just above the vacuum envelope, and positrons enter the trap through a Ti foil of 7μm thickness. Positrons travel along the axis of the Penning traps until they hit the moderator crystal placed below the lower end-cap of the experimental Penning trap. The positron current reaching the crystal was measured by an electrometer. At the beginning of our experiment the measured current was ~2 pA. For the method of trapping positrons discussed in [2], a room-temperature kinetic-energy distribution of moderated positrons is important. Room-temperature distributions of moderated positrons have been reported in the literature for a number of single-crystal metallic moderators. We chose a Cu(111) moderator crystal because of the expected narrow distribution of positrons [21,22], and because it can be annealed at a lower temperature (~900 °C). However, for the experimental results discussed here the moderator crystal was heated only to 350 °C during the vacuum bakeout.

III POSITRON DETECTION

In the experiment, the presence of trapped positrons was verified by three different methods. The positrons were detected by our (a) observing changes in the $^9Be^+$ ion fluorescence due to application of microwaves near the positron cyclotron frequency, (b) detecting the absence of $^9Be^+$ ions in the plasma center in side-view images of the $^9Be^+$ ion fluorescence, and (c) detecting the annihilation radiation after pulsing the accumulated positrons onto the titanium foil above the trap.

The first evidence of positron accumulation was obtained through microwave excitation of the positron cyclotron resonance near 166 GHz. Waveguides carried the microwave radiation into the magnet bore close to the trap center. The microwaves heated the positrons by increasing their cyclotron energy. Through Coulomb interactions the positrons then increased the $^9Be^+$ ion energy which changed the level of the $^9Be^+$ ion fluorescence. The positron cyclotron resonance curve, obtained by sweeping the microwave radiation around 166 GHz, was ~200 kHz wide [3]. We believe this resonance width was probably caused by power broadening. Significant positron excitation was required [3] to observe the resonance because of the weak coupling between the positron cyclotron and the $^9Be^+$ ion motions and the low rate of energy transfer between the positron cyclotron and axial energies in the high magnetic field of our trap [23].

Due to the plasma rotation, ion species with different charge-to-mass ratios tend to centrifugally separate in a Penning trap [24,25]. With positrons and $^9Be^+$ ions, the positrons drift radially inward and the heavier ions outward until both species come to thermal equilibrium and rotate at the same ω_r as a rigid body [25]. In the limit of zero temperature, the edges of each plasma will be sharp (Debye length$\rightarrow$ 0), and the plasmas will completely separate, with the positrons forming a column of uniform density along the trap axis. If the $^9Be^+$ plasma density is significantly below the Brillouin limit, the e^+ and $^9Be^+$ densities are approximately equal and the plasma separation is quite small [25].

Figure 1(b) shows an image of a $^9Be^+ - e^+$ plasma along with the radial dependence of the fluorescence signal. The $^9Be^+$ ion density n_0 is calculated from the rotation frequency ω_r set by the rotating wall. With approximately equal density for both species, the number of positrons in the "dark" column of the plasma image is $n_0 \times V$, where V is the volume of the "dark" region.

If any ions with a mass-to-charge ratio less than $^9Be^+$ are created during the positron accumulation, they will also centrifugally separate and contribute to the size of the non-fluorescing column in the plasma center. With the ^{22}Na source blocked, we deliberately created singly charged light-mass ions by ionizing background gas with a ~15 eV electron beam. From the volume of the central dark region as a function of time, the lifetime of the light-mass ions was measured to be less than 10 hours. Similar measurements were performed after accumulating positrons and are discussed in more detail in the next section. In this case very little change in the volume of the central dark region was observed after the ^{22}Na source was blocked for 12 hours. This indicates that most of the dark central region in Fig. 1(b) is due to positrons rather than impurity ions of light mass.

To further verify that the dark central column in Fig. 1(b) is due to accumulated positrons, we pulsed the $e^+ - ^9Be^+$ plasma onto the 7 μm Ti foil located above the trap and detected the resulting positron annihilation radiation. The positron annihilation radiation was detected with a NaI scintillation crystal mounted 2.5 or

5 cm above the Ti foil. A light pipe coupled the output of the NaI crystal to a photomultiplier tube mounted a few feet above the magnet. The ^{22}Na source is removed from the magnet bore during this procedure.

We attempted to eject all the positrons rapidly compared to the rise time of the NaI crystal scintillation (~300 ns). In this way the scintillation crystal will produce a single pulse, free from background radiation, whose height is proportional to the number of annihilated positrons. The resulting annihilation pulse was recorded on a digital oscilloscope. For a fixed procedure for positron ejection the voltage peak of the output pulse was proportional to the amount of light-mass charge measured from side-view images such as Fig. 1(b). However, changing the ejection procedure by pulsing the positrons with different voltages, or by moving the positrons to the load trap for ejection, produced, in many cases, a different proportionality constant. For some conditions the output annihilation pulse was significantly longer than the scintillator single-event pulse and delayed beyond the scintillator and high-voltage pulse rise-times. This indicated that for these conditions not all the positrons were dumped simultaneously. We believe the reason for this is pick-up and ringing induced by the high-voltage pulse on different trap electrodes. Therefore, to estimate the number of trapped positrons, only annihilation procedures that produced single-event pulses were used.

The NaI crystal detection system was calibrated with a ~37 kBq (1 μC) ^{68}Ge source. Overall we estimate the uncertainty in determining the number of annihilated positrons from the peak of the annihilation pulse to be ~25 %. Figure 2 summarizes the results of positron annihilations done with several different experimental procedures. Systematic variation between the different procedures is

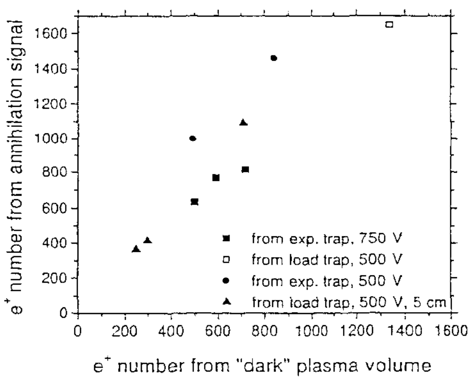

FIGURE 2. Comparison of the number of trapped positrons obtained from the calibrated annihilation signal with the number obtained from the volume of the "dark" plasma column. Measurements were taken with the positrons ejected from different traps, with different voltage pulse heights (500 - 750 V), and with the NaI crystal located 2.5 cm (squares and circles) and 5 cm (triangles) from the Ti foil.

observed. While we do not understand this variation, the positron number determined by the annihilation method should provide a lower limit for the number of trapped positrons. In all cases the positron number measured by annihilation is greater than the number calculated from the volume of the "dark" column. However, the ~40 % difference is on the order of the combined uncertainty of these two positron measurement methods. Therefore we cannot determine with any certainty whether the number of trapped positrons is greater than indicated by the volume of the "dark" column. However the annihilation measurements do support our claim that most of the light-mass charges in images such as Fig. 1(b) are positrons that have centrifugally separated from the Be^+ ions.

Centrifugal separation implies that the positrons are rotating with the same rotation frequency as the Be^+ ions and are cold enough to have approximately the same density. We observed centrifugal separation of the positrons with rotation frequencies up to 1 MHz. For larger rotation frequencies, the radius of the positron column was too small to clearly see separation. In the 6 T magnetic field of this experiment $\omega_r \approx 2\pi\times$ 1 MHz gives positron densities $\sim 4\times 10^9$ cm^{-3}. This is $\sim$ 50 times greater than the highest positron density previously achieved [16].

IV POSITRON ACCUMULATION AND LIFETIME

Because of method's simplicity, we initially attempted to load positrons by following, as much as possible, the method described in Ref. [13] of field ionizing high-Rydberg positronium. The basic idea is that in high magnetic field a fraction of the moderated positrons that leave the moderator crystal combine with an electron to form positronium in a very high Rydberg state at the moderator crystal's surface. After leaving the crystal, the positronium travels into the trap as long as the electric fields between the moderator and trap are not large enough to field-ionize the Rydberg state. The trap potentials are adjusted to give a larger electric field inside the trap capable of field-ionizing the positronium and therefore capturing the positron.

By mimicking this method we were able to accumulate a few thousand positrons. However, our accumulation rate is approximately 3 orders of magnitude lower than that obtained in [13] and limited the total number of positrons loaded into the trap. While both experiments are performed in a high magnetic field (5.3 T in [13] and 6 T in our setup), there were substantial differences in the two setups. In particular, reference [13] used tungsten moderator crystals at cryogenic (4 K) temperatures, compared with the room-temperature Cu moderator used here. They observed that their accumulation rate depended sensitively on the gas absorbed on the surface of the moderator crystal. Heating the moderator while the rest of the trap is at 4.2 K significantly reduced the accumulation rate. Our Cu moderator crystal was baked with the rest of the trap at 350 °C for about 2 weeks, which may have desorbed much of the adsorbed gases. We also plan to accumulate positrons by the method outlined in Ref. [2], where positrons are loaded through Coulomb collisions with trapped $^9Be^+$ ions. Results of this method will be discussed in a future publication.

Figure 3 shows the measured lifetime of the positrons, $^9Be^+$ ions, and light mass impurity ions. The $^9Be^+$ ion and positron lifetimes were measured simultaneously on the same plasma by first accumulating positrons and then blocking the ^{22}Na source and measuring the number of $^9Be^+$ ions and positrons that remained after each day for a week. The trap voltage during the lifetime measurement was -40 V. When the ion and positron numbers were not being measured, the laser cooling and rotating electric field perturbation were turned off. The measured lifetime of the positrons was 8 days and is nearly identical to the measured $^9Be^+$ lifetime. This

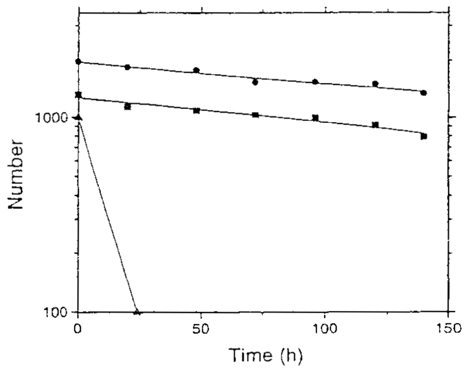

FIGURE 3. Life-time of positrons (solid circles), $^9Be^+$ ions (solid boxes, number shown = actual number ÷ 100) and light impurity ions (triangles)

indicates that the measured positron lifetime could be limited by the trapping lifetime of charged particles in our trap, rather than by annihilation with background gas. We measure the background pressure in our trap to be between 10^{-9} and 10^{-8} Pa. The trap was baked at 350 °C for about 2 weeks and was pumped by a sputter-ion pump and a titanium sublimation pump. For comparison we also show the measured lifetime of light-mass impurity ions. These ions such as H_2^+, H_3^+ or He^+ disappear relatively quickly due to reactions with background gas molecules.

V POSITRON TEMPERATURE ESTIMATE

Centrifugal separation of two-species ion plasmas has been observed and studied in $^9Be^+$-Hg^+ [24], $^9Be^+$-$^{26}Mg^+$ [26], $^9Be^+$-Cd^+ [27], and $^9Be^+$-$^{136}Xe^{q+}$ ($32 \leq q \leq 44$) [28] plasmas. In these experiments, laser-cooling of one ion species resulted in temperatures of less than ~1 K for the other ion species. However, the energy transfer in a $e^+ - {}^9Be^+$ collision is ~1000 times weaker than in these previous sympathetic cooling studies. Because we could not find a more direct method, we used the centrifugal separation of the $^9Be^+$ ions and positrons to place an upper limit of about 5 K on the positron temperature of motion parallel to the magnetic field.

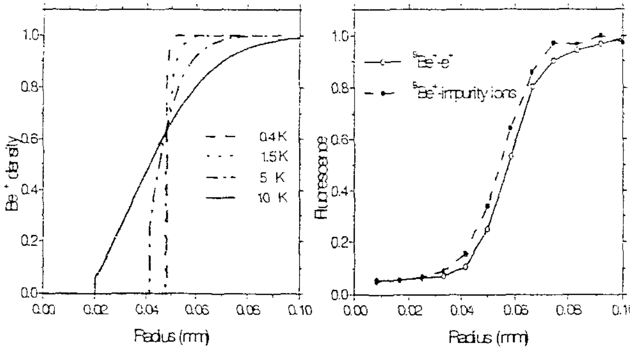

FIGURE 4. (a)Calculated radial variation of the $^9Be^+$ ion density for different positron temperatures, and (b) Measured radial dependence of the fluorescence of scattered laser light for $^9Be^+$ - impurity ion and for $^9Be^+$-e^+ plasmas.

In the 6 T magnetic field of the trap, the positron cyclotron motion is coupled to the room temperature walls (electrodes) of the trap with a ~100 ms time constant. In addition the positron cyclotron motion is collisionally coupled to the positron axial motion, but this coupling becomes exponentially weak when the Larmor radius is less than the distance of closest approach (the strongly magnetized regime). For a 10^9 cm^{-3} positron plasma this energy transfer rate is ~10 Hz for T ~10 K [23]. Therefore we anticipate $T_\perp$ to be ~ 10 K and greater than $T_\parallel$, which is cooled by Coulomb collisions with the laser-cooled $^9Be^+$ ions.

Centrifugal separation has been discussed theoretically by O'Neil [25]. In this case the different charged species were assumed to have the same temperature as required in a global thermal equilibrium state. However, because of the weak thermal coupling between the positrons and $^9Be^+$ ions, the positrons could have a greater temperature than the $^9Be^+$ ions. In order to estimate the effect of the positron temperature on the centrifugal separation we calculated the positron and $^9Be^+$ radial density profiles for an infinitely long column assuming rigid rotation of the plasma but different temperatures. The $^9Be^+$ ions were assumed to be cold (T_{Be^+}=0) and the positron temperature non-zero ($T_{e^+} > 0$). Figure 4(a) shows the results of these calculations for conditions similar to some of the experimental measurements ($\omega_r = 2\pi \times 500$ kHz, positrons/length=1.5×10^5 cm^{-1}). For a given positron temperature, the $^9Be^+$ density makes a sharp jump to a non-zero zero density at a particular radius. This jump is then followed by a gradual increase at larger radii. As the positron temperature increases, the sharp jump becomes smaller and the subsequent increase in the $^9Be^+$ density more gradual.

We compare these calculations with the experimental profiles of the radial variation of fluorescence, or the $^9Be^+$-e^+ ion density (Fig. 4(b)). In the experimental measurements the plasmas had an axial extent that is typically smaller than the overall plasma diameter (see Fig. 1b)). However, the calculations, which are for an infinitely long column, should describe the separation of the species as long as the diameter of the dark region in the $^9Be^+$ fluorescence is smaller than the axial extent of the plasma. We typically worked in this regime. Comparison of the profiles in Figs. 4(a) and (b) shows a measured separation that is significantly sharper than that calculated at 10 K and reasonably consistent with the 5 K separation. Also shown in Fig 4(b) is the measured separation between $^9Be^+$ ions and light mass ions for the same inner column size. From previous studies of sympathetic cooling [24,26–28] we expect the temperature of both species to be less than 1 K. However, because the sharpness of the separation is much worse than calculated for T = 1 K, we believe the profile measurements in Fig. 4(b) are limited by the resolution of the imaging-system optics.

We emphasize that this temperature limit is only for positron motion parallel to the magnetic field. This is because for a strongly magnetized plasma the perpendicular kinetic energy is constrained by a many-particle adiabatic invariant [23]. This modifies the particle distribution function (which is what we measure in Fig. 4(b)) with the result that the Debye length is determined by $T_{\|}$, not $T_{\perp}$ [29].

VI DISCUSSION AND ACKNOWLEDGMENTS

The low accumulation rate limited to a few thousand the number of positrons that could be accumulated. This number needs to be significantly increased for most of the potential applications of cold positrons, such as a source for cold beams. This could be done by combining the sympathetic cooling technique with an established technique for accumulating positrons [12–16]. It is interesting to speculate about the maximum number of positrons that can be sympathetically cooled. A potential limit is the number of ions that can be directly laser-cooled. We can routinely load and laser-cool $\sim 10^6$ $^9Be^+$ ions to temperatures ≤ 10 mK. This ion number is limited by our loading technique rather than by the capabilities of laser-cooling. With a different loading technique non-neutral plasmas of $\sim 10^9$ Mg^+ ions have been laser-cooled to ~ 1 K temperatures [30]. Therefore $\sim 10^9$ positrons, comparable to the current largest number of trapped positrons, could possibly be sympathetically laser-cooled in a Penning trap. This would provide a useful, very cold source of positrons in a room-temperature vacuum system.

Support for this research was provided by the Office of Naval Research. The authors thank Brian Zimmerman and Bert Coursey at the NIST Ionizing Radiation Division for calibrating the activity of the ^{68}Ge source, and Robert Ristenen and Jeffrey Brack for discussion on detecting positron annihilation γ-rays. We thank David Wineland and Tom O'Neil for suggestions through out the experiment and for comments on the manuscript.

REFERENCES

† Also at Institute of Physics, University of Belgrade, Yugoslavia.

* Present address: Ball Aerospace, Boulder, CO 80301.

‡ Present address: Dept. of Physics and Astronomy, Univ. of Delaware, Newark, DE 19716.

1. D. Wineland, C. Weimer, and J. Bollinger, Hyperfine Interac. **76**, 115 (1993).
2. A. Newbury, B. M. Jelenković, J. Bollinger, and D. Wineland, Phys. Rev. A **62**, 023405 (2000).
3. B. Jelenković *et al.*, in *New Directions in Antimatter Chemistry and Physics*, edited by C. M. Surko and F. Gianturco (Kluwer Academic Pubkishers, Dordrecht, The Netherlands, 2001), in press.
4. R. G. Greaves and C. M. Surko, Phys. Plasmas **4**, 1528 (1997).
5. S. Gilbert, C. Kurtz, R. Greaves, and C. Surko, Appl. Phys. Lett. **70**, 1944 (1997).
6. J. Malmberg and T. O'Neil, Phys. Rev. Lett. **39**, 1333 (1977).
7. M. Glinsky and T. O'Neil, Phys. Fluids **B3**, 1279 (1991).
8. G. Gabrielse and the ATRAP Collaboration, Phys. Lett. B **507**, 1 (2001).
9. P. Schwinberg, R. V. Dyck, and H. Dehmelt, Phys. Lett. **81**, 119 (1981).
10. R. Conti, B. Ghaffari, and T. Steiger, Nucl. Instr. Meth. Phys. Res. **A299**, 420 (1990).
11. H. Boehmer, M. Adams, and N. Rynn, Phys. Plasmas **2**, 4369 (1995).
12. L. Haarsma, K. Abdullah, and G. Gabrielse, Phys. Rev. Lett. **75**, 806 (1995).
13. J. Estrada *et al.*, Phys. Rev. Lett. **84**, 859 (2000).
14. T. Murphy and C. Surko, Phys. Rev. A **46**, 5696 (1992).
15. C. Surko, S. Gilbert, and R. Greaves, in *Non-neutral Plasma Physics III*, edited by J. Bollinger, R. Spencer, and R. Davidson (AIP, New York, 1999), p. 3.
16. R. Greaves and C. Surko, Phys. Rev. Lett. **85**, 1883 (2000).
17. W. Itano, L. Brewer, D. Larson, and D. Wineland, Phys. Rev. A **38**, 5698 (1988).
18. J. Bollinger and D. Wineland, Phys. Rev. Lett. **53**, 348 (1984).
19. L. Brewer *et al.*, Phys. Rev. A **38**, 859 (1988).
20. X.-P. Huang, J. Bollinger, T. Mitchel, and W. M. Itano, Phys. Rev. Lett. **80**, 73 (1998).
21. C. Murray and A. M. Jr, Solid State Commun. **34**, 789 (1980).
22. R. Wilson, Phys. Rev. B **27**, 6974 (1983).
23. M. E. Glinsky, T. M. O'Niel, and M. N. Rosenbluth, Phys. Fluids B **4**, 1156 (1992).
24. J. Larson, J. Bergquist, W. Itano, and D. Wineland, Phys. Rev. Lett. **57**, 70 (1986).
25. T. O'Neil, Phys. Fluids **24**, 1447 (1981).
26. J. Bollinger *et al.*, IEEE Trans. Instr. Measurement **40**, 126 (1991).
27. H. Imajo *et al.*, Phys. Rev. A **55**, 1276 (1997).
28. L. Gruber *et al.*, Phys. Rev. Lett. **86**, 636 (2001).
29. D. H. Dubin and T. O'Niel, Phys. Rev. Lett. **60**, 511 (1988).
30. E. Hollmann, F. Anderegg, and C. Driscoll, Phys. Rev. Lett. **82**, 4839 (1999).